Hexagonal Boron Nitride Platelet-Based Nanocoating for Fire Protection

Anne-Lise Davesne, Simone Lazar, Séverine Bellayer, Shuang Qin, Jaime C. Grunlan, Serge Bourbigot, Maude Jimenez

Hexagonal Boron Nitride Platelet-Based Nanocoating for Fire Protection

Anne-Lise Davesne,[†,#] Simone Lazar,[‡,#] Severine Bellayer,[†] Shuang Qin,[§] Jaime C. Grunlan,[*,‡,§,∥] Serge Bourbigot,[†] and Maude Jimenez[*,†]

[†]Unité Matériaux et Transformations (UMET) - CNRS UMR, University of Lille - ENSCL, 8207 Av. Mendeleiev - CS 90108, 59652 Cedex Villeneuve d'Ascq, France

[‡]Department of Chemistry, [§]Department of Materials Science and Engineering, and [∥]Department of Mechanical Engineering, Texas A&M University, College Station, Texas 77843, United States

Supporting Information

ABSTRACT: Because of its widespread use in furniture upholstery, buildings, and transportation, the flame retardancy of flexible polyurethane foam is a matter of great concern. In an effort to impart fire resistance in an environmentally benign manner, hexagonal boron nitride (h-BN) nanosheets were dispersed by an aqueous route and deposited as a single bilayer with polyethylenimine (PEI) on flexible polyurethane foam by using layer-by-layer assembly. Butane torch exposure and cone calorimetry show that the nanocoating performs similarly to vermiculite clay (VMT), while in situ quantitative gas phase analysis reveals that carbon monoxide emissions are lower with h-BN. The PEI/h-BN system also maintains foam flexibility and protects against weathering, preventing yellowing. These combined properties make the use of h-BN nanoplatelets an interesting alternative for the protection of polyurethane foam (and perhaps other flammable substrates).

1. INTRODUCTION

Polymers contribute to our overall quality of life, but their high flammability is a major concern. Loss of life and property damage from fires are a continuous reminder of the need to find protective treatments that limit flammability. The acoustic and thermal insulation properties, resiliency, and strength make flexible polyurethane foam (PUF) the material of choice for furniture upholstery and building construction.[1] Despite these benefits, PUF is a major contributor to domestic fires, as it burns very quickly, and its combustion is accompanied by dripping and emission of highly toxic gases.[2,3] Most fire retardants are halogenated molecules, which are quite efficient but are under scrutiny because of the pollution they generate and their health hazards.[4] In an effort to impart more environmentally benign flame-retardant behavior to foam, thin coatings, particularly water-based multilayer coatings deposited using layer-by-layer (LbL) assembly, have attracted tremendous attention due to their good efficacy.[5] LbL-deposited nanocoatings can uniformly cover complex three-dimensional substrates, such as polyurethane foam. Thin nanocomposite coatings, composed of polyelectrolytes and nanoparticles, have been abundantly studied for this purpose. For example, halloysite,[6] titanate nanotubes,[7] layered double hydroxides,[8] graphene,[9] and carbon nanotubes[10] have all been deposited on the surface of polyurethane foam to improve fire resistance.

A key limitation of layer-by-layer coatings is found in the high number of processing steps required to obtain sufficient thickness and therefore significant efficacy, despite its numerous advantages. Recent studies have focused on reducing processing time,[11] but a more promising approach is the use of high performance nanoparticles. These materials have been found to exhibit exceptional fire protection with only a single bilayer nanocoating, especially when used with a binding polymer.[12,13] Two-dimensional materials, such as vermiculite or graphene, have proven to be very effective in imparting fire retardancy when used in thin coatings.[9] Cain et al. combined vermiculite (VMT) clay platelets with polyethylenimine, which reduced the peak heat release rate (pkHRR) by 54% and the total heat release (THR) by 8% with only one bilayer.[13]

Boron nitride has been used for applications in high-temperature equipment and as a lubricant due to its high thermal stability and conductivity, electrical insulation properties, and chemical inertness.[14−16] Hexagonal boron nitride (h-

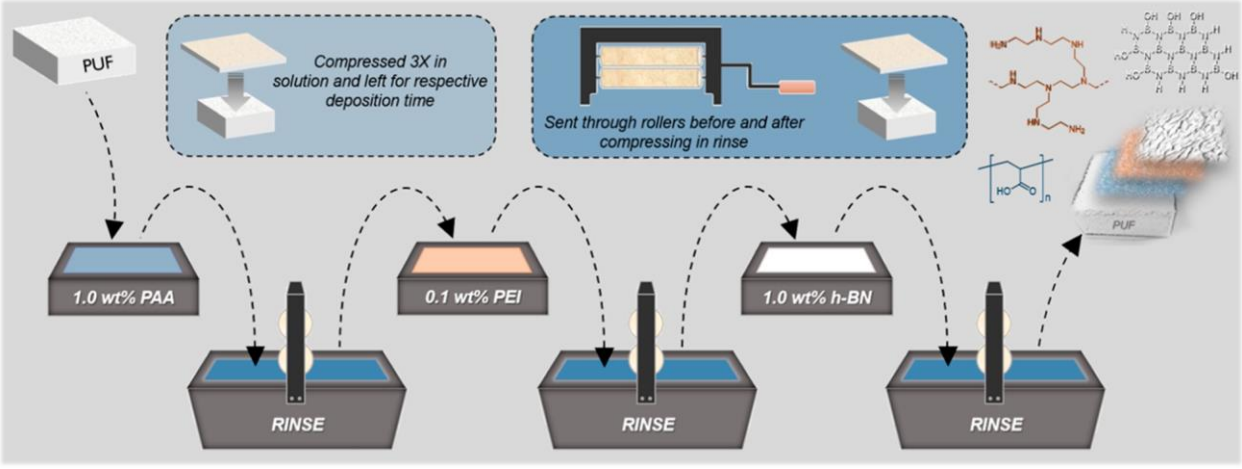

Figure 1. Schematic of the layer-by-layer process used to coat polyurethane foam samples.

BN) is an analogue of graphite with boron and nitride atoms replacing carbon atoms and can be exfoliated to yield nanosheets. Boron nitride's anisotropic thermal conductivity and high thermal stability make it very promising in terms of thermal management.[17−23] Additionally, it has been used for corrosion protection,[24−26] gas barrier,[27,28] and electronic applications.[15,29] Despite these beneficial properties, the hydrophobicity of these nanosheets has restricted their use in aqueous processes. Lin et al. overcame this limitation after demonstrating that h-BN can be hydrolyzed through a sonication-assisted process.[30] Surprisingly, the opportunity to use h-BN nanoplatelets in LbL-deposited coatings has been scarcely examined by the scientific community.[31,32] Despite its promising application in the field of fire retardancy, researchers are only beginning to mention their use for this purpose.[33]

In the present work, boron nitride nanoplatelets were prepared via an aqueous procedure, resulting in hydroxylated h-BN nanosheets. These exfoliated nanosheets were then deposited in a single bilayer on polyurethane foam, paired with polyethylenimine (PEI), by using layer-by-layer assembly to create a high performance fire-retardant coating. Fire performance was evaluated using a torch test and mass loss cone calorimetry and compared to the performance of the well-known PEI/VMT system.[13] The single PEI/h-BN bilayer outperformed PEI/VMT, reducing the peak of heat release rate of PUF by 55%. Additionally, the PEI/h-BN coating maintained the whiteness of the flexible foam and did not stiffen it. This study demonstrates a very simple, environmentally benign nanocoating for protecting polyurethane foam from both UV and fire.

2. EXPERIMENTAL SECTION

2.1. Materials. Hexagonal boron nitride powder (h-BN, 98%, ∼1 μm), branched polyethylenimine (PEI, 25000 g mol^{-1}), and poly(acrylic acid) [PAA, 100000 g mol^{-1}, 35 wt % in water] were purchased from Sigma-Aldrich (Milwaukee, WI). Microlite 963++ vermiculite clay (VMT, 7.8 wt % in water) was purchased from Specialty Vermiculite Corp (Cambridge, MA). Open-cell polyether-based polyurethane foam (type 1850, 1.75 lb ft^{-3} density) was purchased from Future Foam (High Point, NC). A dilute solution of 70% nitric acid, purchased from Sigma-Aldrich, was used to adjust the pH of the PAA solution. All products were used without further purification and were prepared by using 18 MΩ deionized (DI) water.

2.2. Layer-by-Layer Deposition. For the PEI/h-BN system, a 0.1 wt % PEI solution (unaltered pH 11) was paired with a 1.0 wt % h-BN dispersion in water (unaltered pH 8). The h-BN dispersion was sonicated for 8 h by using a 5510 Branson ultrasonic bath. The same concentrations were used for the PEI/VMT control system (1.0 wt % VMT dispersion, unaltered pH 8) for direct comparison. Prior to treatment, polyurethane foam samples (10 × 10 × 2.5 cm^3) were rinsed with DI water and dried in an oven at 70 °C. A 1.0 wt % solution of PAA (adjusted to pH 2 using 2 M nitric acid, magnetically stirred to ensure proper dissolution) was used via hydrogen bonding as a primer layer to the substrates by immersing the samples for 1 min. Afterward, the foam was soaked in the PEI solution for 5 min before being exposed to the h-BN dispersion for 5 min to complete the coating. After each coating step, the foam was compressed three times in a given solution and then rinsed thoroughly with DI water. The samples were wrung out by using mechanical rollers before submersion in the next solution. The coated samples were dried overnight in an oven at 70 °C before characterization. The same layer-by-layer process, as shown in Figure 1, was used to coat PEI/VMT samples.

2.3. Coating Characterization. The surface morphology of the uncoated and coated polyurethane samples was observed by using a JEOL JSM-7500 field-emission scanning electron microscope (SEM) (Tokyo, Japan). The samples were coated with 5 nm of platinum/palladium before imaging. Boron X-ray mapping was performed on cross sections of the treated foam by Electron Probe Micro-Analysis at 10 kV on a CAMECA SX100 (Gennevilliers, France). A FEI Tecnai G2-20 twin transmission electron microscope (TEM) (Hillsboro, OR) was used to reveal the nanostructure of the coating on PUF. The thermal degradation behavior of neat PUF and PEI/h-BN-coated PUF was evaluated by using a Discovery thermogravimetric analyzer (TGA) from TA Instruments (New Castle, DE). The analyses were performed between 40 and 800 °C at a heating rate of 10 °C/min under air and nitrogen atmospheres. The purge flow (nitrogen) and the sample purge flow (air or nitrogen) were set respectively at 15 and 50 mL/min. The gases that evolved during the test were analyzed with a Nicolet iS10 Fourier transform infrared spectrometer (FTIR) linked to the TGA. The instrument was equipped with a gas cell (10 cm path length with KBr windows) set at a temperature of 215 °C, and the transfer line was heated to 225 °C to avoid condensation. The chemical structure of the PEI/h-BN coating was investigated by ^{11}B solid state magic angle spinning nuclear magnetic resonance (MAS NMR), performed at 256.7 MHz on an Advance II 800 MHz spectrophotometer (Bruker, Billerica, MA). The analysis was performed with 128 scans in a 3.2 mm probe at MAS of 20000 Hz. The standard used was $NaBH_4$, and simulations of the spectra were performed using DMFit2015.[34]

2.4. Fire Behavior. PEI/h-BN- and PEI/VMT-coated polyurethane foam samples (5 × 5 × 2.5 cm^3) were subjected to a small scale torch test and compared to the uncoated control. The samples were placed on a wired grid and exposed to the flame (about 1400 °C

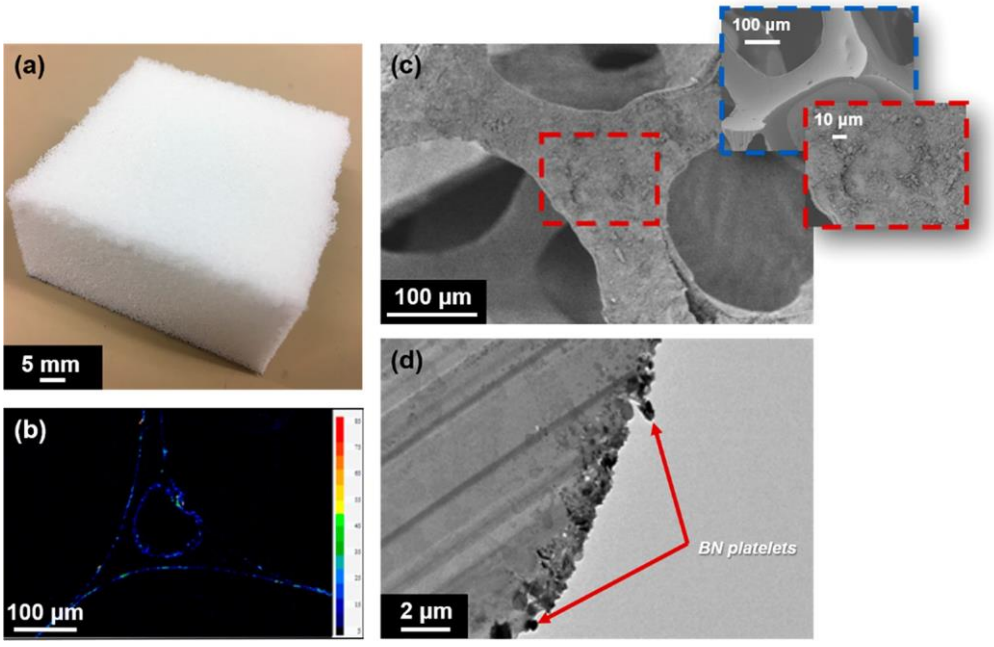

Figure 2. (a) Digital image, (b) Boron X-ray mapping, (c) low-magnification SEM image, and (d) TEM cross-sectional micrograph of one bilayer of PEI/h-BN-coated PUF (the inset outlined in blue is an SEM image of neat PUF for comparison).

measured by a thermocouple located in the center of the flame) of a butane hand torch (Lifebee Professional kitchen blowtorch) for 10 s. Flame resistance was evaluated by weighing the samples before and after testing and calculating mass loss. The morphology, nanostructure, thermal degradation behavior, and chemical structure of the residues from the torch test were analyzed by using the tools described in section 2.3. Resistance to a radiative fire scenario was tested by using a mass loss cone (MLC) calorimeter (Fire Testing Technology (FTT), East Grinstead, UK) under 35 kW/m^2 heat flux. This instrument is similar to that used in ASTM E1354, except that it relies on a thermopile in the chimney to obtain heat release rates instead of using the oxygen consumption principle. The PEI/h-BN- and PEI/VMT-coated foam were compared to untreated samples. The samples were wrapped in aluminum foil, leaving only the upper surface exposed, and placed horizontally under the heater at a distance of 25 mm from the cone base. Samples were weighed before and after testing to determine the mass loss. The different characteristics of the combustion behavior were recorded, namely, the time-to-ignition (TTI [s]), the peak heat release rate (pkHRR [kW/m^2]), and the total heat release (THR [kW/m^2]). Tests were performed in duplicate to ensure repeatability of the results. The gases evolving during the test were carried to a Fourier transform infrared spectrometer (FTIR, Antaris Industrial Gas System, Thermo Fisher, Waltham, MA) by a transfer line heated to 200 °C to avoid condensation. The instrument was equipped with a gas cell (2 m long optical pathway, chamber filled with dry air, two KBr windows) set at a temperature of 186 °C and pressure of 653 Torr.

2.5. Mechanical Properties and Weathering. Tensile tests were performed using an Instron 4466 Universal testing instrument (Norwood, MA) with PEI/h-BN- and PEI/VMT-coated foam (40 × 10 × 3 mm^3) and uncoated control foam. The machine was equipped with a 100 N load cell, and the tests were performed with a 10 mm/min speed at ambient temperature. Accelerated weathering under UV-A light of the PEI/h-BN- and PEI/VMT-coated foam, as well as the uncoated foam, was performed in a QUV accelerated weathering tester from Q-lab (Westlake, OH). The chamber is equipped with four UV lamps (351 nm), and the irradiance is set at 0.76 W/m^2. The samples were exposed to cycles of 4 h light (UV irradiation turned on) followed by 4 h dark (UV irradiation turned off) at 50 °C. The aging time was 56 h, which is equivalent to seven light/dark cycles. Natural weathering was also performed on uncoated and coated PUF. Samples were set on the ledge of a shut window found inside the laboratory for 7 days under ambient conditions. It should be noted that this natural weathering experiment was conducted in June 2018 in Villeneuve d'Ascq, in northern France.

3. RESULTS AND DISCUSSION

3.1. Exfoliation and Assembly of h-BN Nanosheets. Hexagonal boron nitride is composed of nanosheets held together in a graphitic structure via weak van der Waals interactions. The boron and nitrogen atoms present in these nanosheets are covalently linked together and arranged in a honeycomb-like structure (similar to graphene), resulting in stacked nanosheets that form a hexagonal crystalline structure.[15,35] Exfoliation can be easily achieved through sonication in solvents that match its surface energy, such as isopropyl alcohol and DMF,[14] but the hydrophobicity of h-BN makes exfoliation in water difficult, resulting in low concentration and fast reaggregation. To overcome this problem, Lin et al. demonstrated that these nanosheets can be successfully dispersed in water by using sonication-assisted hydrolysis, which reduces the size of the nanosheets and introduces hydroxyl groups on the edges after prolonged sonication.[30] Figure S1 compares the FTIR spectra of h-BN, before and after 8 h of exfoliation. The absorptions at 1327 and 760 cm^{-1} correspond to the B−N stretching and B−N−B bending for pristine h-BN, respectively.[36] After exfoliation, a broad absorption around 3330 cm^{-1} is observed due to the hydroxyl edge functionalization, while the two absorptions characteristic of h-BN broaden and shift toward a lower frequency due to hydrogen-bonding interactions.

This aqueous dispersion of exfoliated nanosheets was used for deposition on polyurethane foam, which was first coated with a thin layer of PAA through hydrogen bonding. A layer of h-BN nanosheets was then deposited by means of an intermediate PEI layer, also held together by hydrogen bonds between PAA and exfoliated h-BN, as well as Lewis adducts formed between the lone pair boron acceptors and

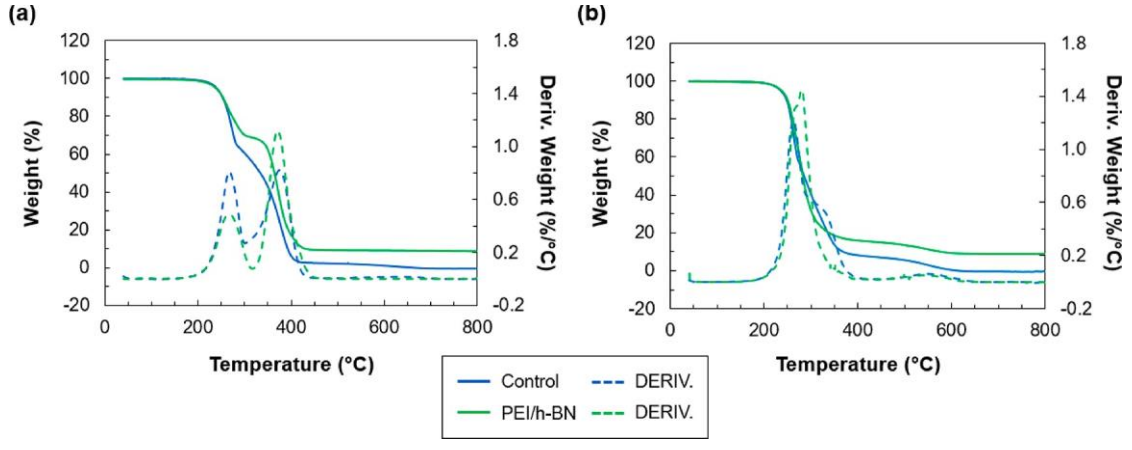

Figure 3. Thermogravimetric analysis of uncoated PUF and PEI/h-BN-coated PUF (a) under nitrogen and (b) air atmospheres.

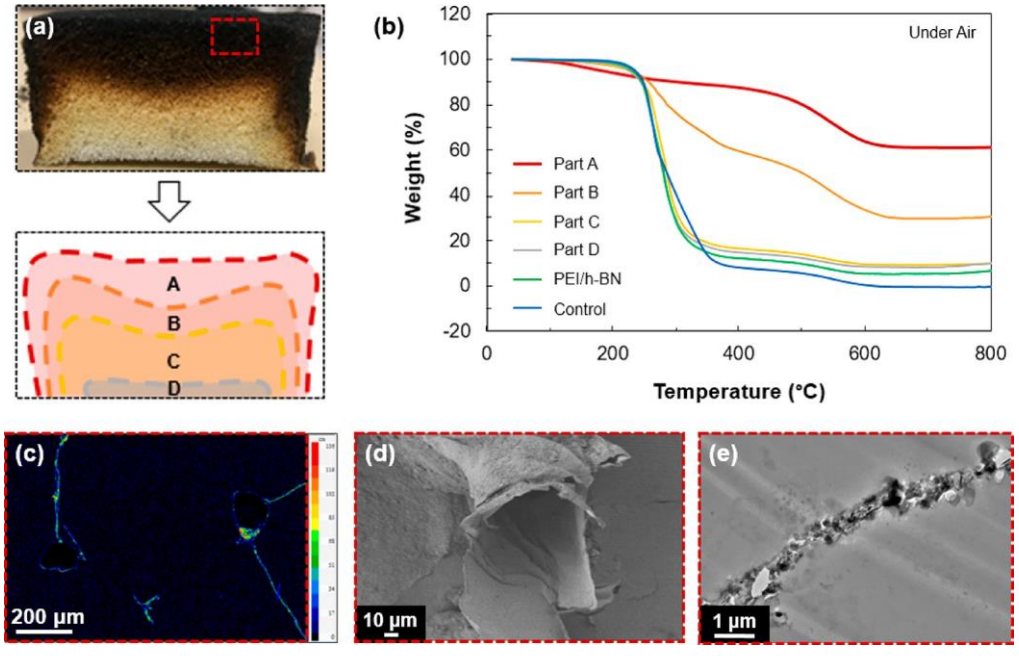

Figure 4. (a) Cross-sectional image of the PEI/h-BN-coated PUF after torch testing with the positions of the four parts (A−D) of the residue, studied by (b) thermogravimetric analysis compared to uncoated and PEI/h-BN unburnt coated PUF. (c) EPMA B X-ray mapping, (d) SEM image, and (e) TEM cross-sectional micrograph of the charred portion of PEI/h-BN-coated PUF after torch testing.

electron-rich amine functionalities of PEI.[37−39] The same process was used to deposit a single bilayer of PEI/VMT for comparison. From an aesthetic point of view, the PEI/h-BN system did not change the color of the white polyurethane foam (Figure 2a), whereas a homogeneous beige coloration was observed after the deposition of the PEI/VMT bilayer. Both systems resulted in very little weight gain, but the PEI/h-BN bilayer is thicker than PEI/VMT (11.1 ± 0.2 vs 2.3 ± 0.2 wt % added, respectively).

Electron probe microscopy, with boron X-ray mapping, demonstrates the homogeneous and conformal deposition of PEI/h-BN (Figure 2b). Boron distribution is quantified on a color scale ranging from dark blue (low concentration of boron atoms) to bright red (high concentration of boron atoms). Signals corresponding to the presence of boron are found to be homogeneously distributed in the dark blue range of the scale, tracing an outline of the foam's cellular structure. Significant quantities of boron atoms were detected and are localized on the cell walls of the three-dimensional PUF structure. SEM images confirm this observation, as shown in Figure 2c, which shows the typical open-cell morphology of the foam. The textured surface of the cell walls, in contrast with the smooth morphology of the uncoated foam, shows that the coating is deposited conformally throughout the cells, with no change in the porosity. A TEM cross-sectional image depicts the two-dimensional h-BN platelets as round shaped, appearing slightly darker than the polymeric material (Figure 2d). The platelets appear to be embedded in the PEI matrix that follows the PUF structure with no preferential spatial arrangement, contrary to systems constituted of clay nanoplatelets.

3.2. Thermal Stability. The thermal stability of the PEI/h-BN system was investigated by using thermogravimetric analysis, under air and nitrogen atmospheres, as shown in Figure 3. Under nitrogen, the uncoated foam exhibits two clear degradation steps that are attributed to the decomposition of hard segments of polyurethane, followed by the decomposition of soft segments.[6] This can be seen around 270 and 370 °C (maximum degradation rate) for both the control and PEI/h-

BN-coated foam, respectively. Under air, the uncoated foam also undergoes two degradation steps. Almost all the polyurethane is consumed during the first step (93% mass loss), occurring at ~260 °C, resulting in a stable residue that further degrades at around 550 °C. The presence of the nanocoating slightly delays oxidation, with the maximum degradation rate temperature being 280 °C, but the apparent degradation pathway is unchanged. Although h-BN has high intrinsic thermal conductivity, the coating is likely too thin to accelerate heat transfer and alter the degradation of the polyurethane. In both nitrogen and air, a residual mass around 7% is observed for the coated samples, while there is no residue left behind from the control foam at 800 °C. The presence of the nanocoating slightly delays the foam pyrolysis or its oxidation, but it does not change its degradation behavior. It can be postulated that only h-BN platelets remain at the end of the TGA experiment, with all organic matter having been degraded.

3.3. Fire Behavior. The flame retardancy of foam was evaluated by exposing samples to a butane torch test for 10 s, which provides essentially the same information as the UL-94 test that is commonly used to test dense, nonporous bars or plaques. This test serves as a quick comparison of the PEI/h-BN system with the PEI/VMT coating. Upon exposure to the flame, the uncoated control foam completely degrades, and melt dripping is observed. The addition of a PEI/h-BN bilayer is enough to completely suppress this phenomenon, similar to what is observed with PEI/VMT. Both coated foam samples retain their macroscopic open-cell structure with little shrinkage. The h-BN coating is comparable to the clay coating, with a slightly higher mass loss of 48.9 ± 1.1% (PEI/VMT is 42.1 ± 1.1%). An image of the cross section of the residue of the PEI/h-BN treated foam shows that only the outer layer of the sample was charred (Figure 4a), as indicated by its black color. The color then turns from dark brown to a faded yellow and then white for the inner core. This implies a degradation gradient within the sample. To quantify this observation, the residue was divided into four parts (A−D), with each part analyzed by thermogravimetric analysis to measure the residual organic content (Table 1). Because h-BN nanoplatelets do not degrade during the test, as shown in Figure S1, the mass loss observed can be attributed to residual organic matter. The TGA of parts C and D in Figure 4b almost perfectly fit the curve of the unburnt PEI/h-BN treated foam, suggesting that the polyurethane foam was protected by the upper layers and did not degrade during the torch test. The only indication of some damage to the polymer is the faded yellow coloration of part C, which implies that it begins to slightly oxidize because of the heat.

Table 1. Organic Content of Varying Depths of the Torch Test Residue

sample	residue[a] (%)	organic content (%)
part A	61.1	38.9
part B	30.6	70.1
part C	10.1	90.6
part D	9.9	91.7
PEI/h-BN	6.8	94.6
control	0	100

[a]Residues at the end of TGA testing are also indicated and are characteristic of the mineral content of the samples.

Parts A and B in Figure 4 exhibit different degradation behavior upon torch exposure. Part B degrades in two steps: the first one being at the same temperature as the unburnt polyurethane and the second one corresponding to the decomposition of the stable char. This suggests that some of the neat polymer did not degrade during the torch test. Polyurethane in part A was completely degraded and turned into a stable char during the torch test, which is shown by the absence of degradation around 300 °C and by the decomposition step around 500 °C in Figure 4b. The increasing residue at 800 °C shows the evolution of the mineral/organic ratio of the char. The organic content is minimal in part A but increases to the level of the unburnt treated foam in parts C and D.

The morphology of the char was investigated by using electron microscopy. The PEI/h-BN-coated PUF retains its open-cell structure as can be seen in the boron X-ray mapping of the cross section of the char by using EPMA (Figure 4c). The boron within the nanoplatelets trace the boundaries of the structure of the foam even after torch testing. The SEM image in Figure 4d confirms this observation, since the residue is composed of an empty shell, in which the boundaries are defined by the coating and remain in place during the test. This means the undegraded coating remains on the cell walls during the torch test, while the polymer decomposes, leaving a hollow mineral shell that forms a skeleton with an open cell structure. Additionally, the nanocoating provides a support for the polymer to char on, preventing the sample from collapsing and crumbling, all while shielding the inner part of the sample.

The stability of the platelets nanostructure during the torch test was investigated to determine whether they experienced any physical or chemical modifications. As can be seen in Figure 4e, exposure to a torch flame did not change the organization of the nanocoating. Moreover, there is no difference between the nanostructure of the unburnt and burnt coating, which shows impressive thermal stability of the nanoparticles. The stability of these nanoparticles is also confirmed by ^{11}B solid-state NMR analysis (Figure 5). Boron is an atom that has a 3/2 spin, meaning quadrupolar interactions within the sample during NMR analysis generate wide and asymmetric peaks. Raising the magnetic field to 800 MHz cancels weak quadrupolar interactions (of tetracoordinated atomic structures), but in the case of tricoordinated boron, the quadrupolar constant is too high to cancel and the resonance band exhibits the "wavy" line shape shown in the spectra. The simulation of the spectra of pristine h-BN platelets shows a single peak around 30 ppm, which is characteristic of tricoordinated boron and corresponds to BN_3 sites (see Figure S2a).[40−42] The spectra of the coated h-BN foam is very similar to that of the h-BN powder. Moreover, no difference can be seen with the burnt residue, which means the h-BN did not degrade during the test. The absence of other peaks in the simulated spectra (see Figure S2b,c) suggests that the nanoparticles did not react nor interact with their surrounding matrix during the fire test.

3.4. Cone Calorimetry. Uncoated, PEI/VMT-coated, and PEI/h-BN-coated PUF were evaluated by cone calorimetry. All three samples caught fire immediately when exposed to the 35 kW/m^2 heat flux. The entire uncoated sample was consumed quickly, whereas a foamlike residue remained for both coated samples. Both systems maintain ~20% of the initial mass, despite the differences in appearance (Figure 6a). After cone calorimetry, the PEI/VMT sample's surface is gray, while the

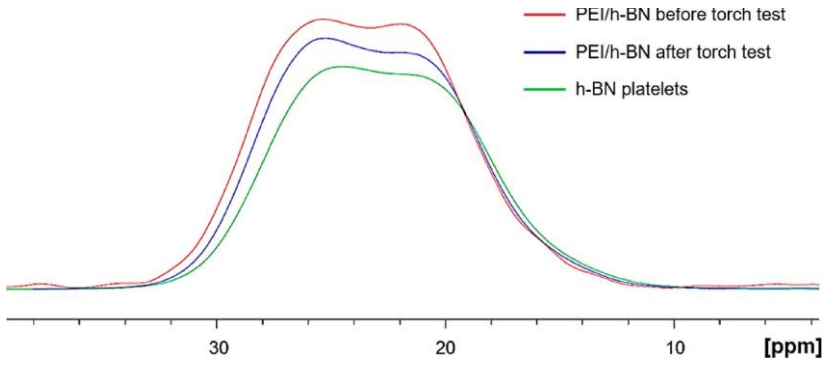

Figure 5. ^{11}B solid-state NMR spectra of PEI/h-BN-coated PUF before and after torch testing compared with pristine h-BN platelets. The peaks are centered around 26 ppm.

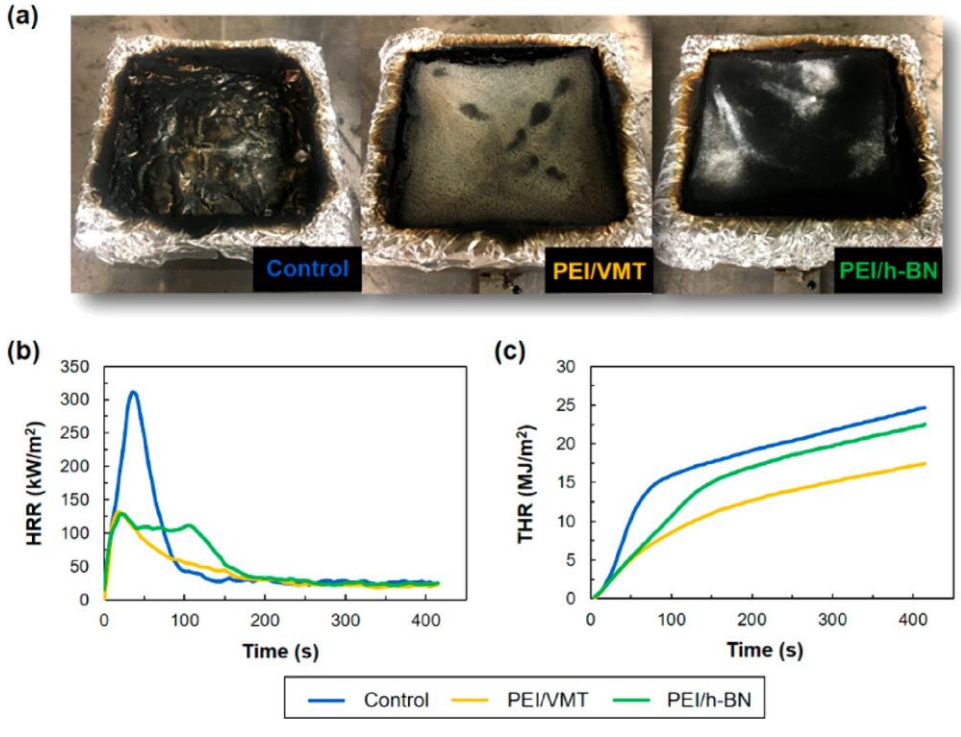

Figure 6. (a) Digital images of the foam residue after cone calorimetry as well as (b) heat release rate and (c) total heat release as a function of testing time for uncoated, PEI/h-BN-coated, and PEI/VMT-coated PUF.

PEI/h-BN sample's surface is black with disparate white spots. These coated foam samples greatly improve the stability of the PUF, reducing the pkHRR by more than 50% (51% for PEI/VMT and 54% for PEI/h-BN). These two values are within a 10% error range, meaning both systems have a very similar effect on the pkHRR. It should be noted that the time to pkHRR is shortened, from approximately 40 to 20 s, for both the coated systems (Figure 6b). Figure 6c shows that both samples have a reduced total heat release compared to the neat foam. The only difference between the two coatings is the slight reduction of THR brought about by the PEI/VMT system, which is not seen with the boron-containing coating (Table S2).

To gain a better understanding of the PEI/h-BN coating's mode of action, the gases released during cone testing were quantified by in situ FTIR analysis. Water (H_2O), carbon dioxide (CO_2), nitric oxide (NO), and carbon monoxide (CO) are released during the combustion of the uncoated PUF (Figure 7). Traces of HCN and methane are also detected, but not in significant quantities. The evolution of all four major gases follows almost exactly the HRR curve (Figure 6b). In regard to H_2O, CO_2, and NO, the treated foam samples both release the same gases as the uncoated control, but in much lower quantities. The peak of gas released during the combustion is reduced by more than 50% for both coated systems. It should be pointed out that this behavior occurs faster than what is observed for the control foam. The release of water, carbon dioxide, and nitric oxide during combustion follows the curve of heat release rate and is negligible after flame-out. For these gases, the PEI/VMT-treated foam is a little more advantageous than the h-BN-coated one. Even so, the boron-containing foam releases far less CO than the PEI/VMT system, suggesting that h-BN may provide a better thermal barrier (due to thicker coating) that suppresses the transfer of decomposed volatiles, more so than the VMT platelets.[43] Surprisingly, for both treated foams, a large peak can be observed just after flame-out. This phenomenon, which is not seen in the control foam, is very pronounced in the case

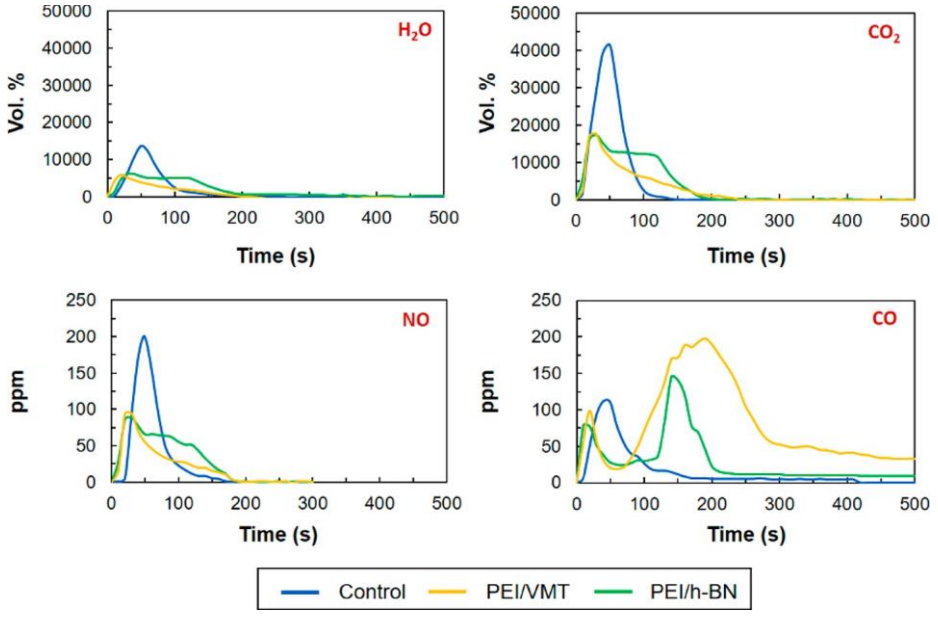

Figure 7. Quantitative in situ FTIR analyses of the gases released during cone calorimetry.

of the PEI/VMT-coated foam, which can be attributed to an incandescence phenomenon. Indeed, a peak at 190 ppm at 200 s is observed, whereas for the PEI/h-BN-coated foam, the curve peaks at 140 ppm at 150 s. In this case, the h-BN coating has a clear advantage, since lower quantities of CO are released initially compared to the clay-containing system.

In a radiative fire scenario, LbL-treated foam reduces the pkHRR by more than 50%, while also reducing the THR and the quantities of water, carbon dioxide, and nitric oxide released. Both coatings have similar performance, but larger quantities of carbon monoxide evolve compared to the control because of incandescence. This undesirable release of gas is attenuated in the PEI/h-BN system. Additionally, the coating provides structural integrity to the material, preserving the open-cellular structure of the foam. The increased mass residue demonstrates the improved char-forming ability of the material due to its structural integrity, a phenomenon that has been previously reported.[44]

3.5. Mechanical Properties. The foam stress−strain behavior was evaluated to determine the change in mechanical properties brought on by the deposited coatings when compared to the uncoated control (Figure 8). Samples were run in triplicate, and their average elongations at break are reported in Table S2. The curves shown in Figure 8 are representative examples of each type of foam. The h-BN-treated foam is only modestly stiffer than the control, with the elongation at break decreasing by 22.5%. This is desirable since protective coatings should have as little impact as possible on the functional properties of the material at hand. Flexible foam is typically used as cushioning in upholstered furniture. The VMT-based nanocoating has a much greater impact on the stiffness and elongation at break (−42.7%) of the foam. The stiffening of both treated foam samples can be attributed to the presence of the nanocoating. It is speculated that the stiffness enhancement of the PEI/VMT-coated foam is due to the highly organized platelets within the polymer−clay system. It has been shown that this organization maximizes the interaction between the polymer and the clay platelets, which constrains the polymer chains and enhances the load transfer between the two components of the coating.[45,46] The countereffect of this improvement of tensile strength is that the nanocomposite is more stiff. As shown in Figure 2d, the h-BN nanocoating lacks this high level of organization, which explains why the stiffening is less pronounced for the PEI/h-BN-coated foam.

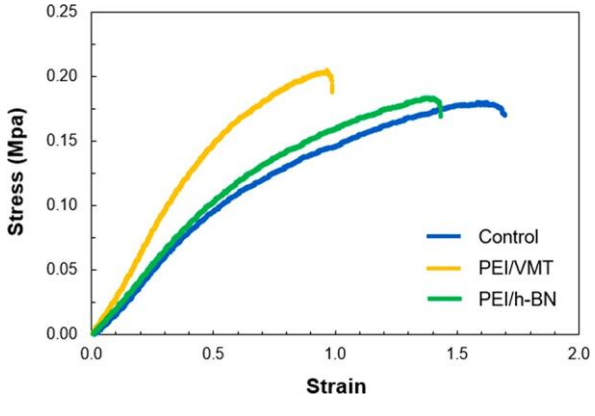

Figure 8. Stress as a function of strain for uncoated, PEI/VMT-coated, and PEI/h-BN-coated PUF.

3.6. Aging. Natural aging tests were conducted on neat, PEI/h-BN-coated, and PEI/VMT-coated PUF to evaluate weathering resistance. Flexible polyurethane foam is generally used for indoor purposes, so samples were placed on a ledge behind a closed window, while the curtains remained open, allowing adequate exposure to sunlight. After 7 days, the color of the foam changes from white to yellow, whereas the PEI/h-BN-coated foam remains white (Figure 9a). As previously mentioned, the PEI/VMT coating imparts a beige color to the foam from the natural coloring of the clay. This color darkens when exposed to the environment, meaning that there is no significant improvement compared to the control. An artificial accelerated aging test under UV light was conducted on the control and PEI/h-BN foam to further evaluate UV resistance. Figure 9b shows images of foam samples before and after testing. After only one cycle, the uncoated foam begins to turn

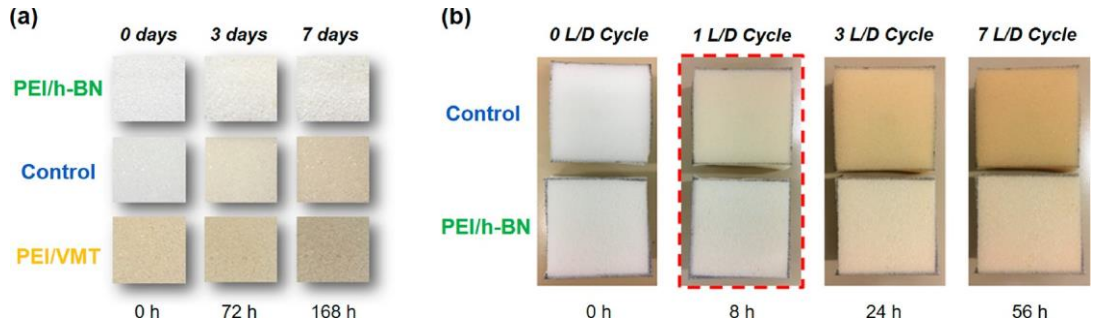

Figure 9. Aging results from (a) the natural environment and (b) UV light, in terms of discoloration. Notation: 4 h light (L); 4 h dark (D).

a yellowish color, characteristic of degradation of the polymer chains, which create chromophore units.[47] The change in color intensifies as the number of testing cycles increases. The change in color is much less dramatic for the PEI/h-BN-coated foam. Yellowing of the foam is not visible until after three cycles, which means that the polymer is protected from degradation for a longer period of time. Additionally, the change in color is not as dramatic, remaining lighter compared to the control foam. This UV protective behavior may be attributed to the high surface-to-volume ratio (i.e., thicker coating/larger weight gain) of the deposited boron nanosheets compared to vermiculite clay.[48] It should be noted that PEI by itself yellows over time and is not contributing to the anti-yellowing behavior observed here.

4. CONCLUSIONS

In this work, h-BN platelets were successfully exfoliated to enable aqueous processing and utilization in layer-by-layer assembly on flexible polyurethane foam for fire protection purposes. The nanoparticles were conformally deposited on the cell walls of the foam with polyethylenimine in a single ~82 nm thick bilayer. Against a butane torch, the PEI/h-BN coating is found to act as an inflammable shield that protects the inner parts of the sample, resulting in a degradation gradient through the foam's thickness. In a cone calorimeter, the coating is found to reduce the pkHRR by 54% and the THR by 20%, while also demonstrating the ability to reduce the amount of gas emitted. This behavior is believed to be due to the improved char formation of the h-BN, thereby reducing the amount of gaseous products emitted. This is an advantage that is not observed when comparing gas emissions to a well-known PEI/VMT coating. Additionally, the PEI/h-BN coating protects the polyurethane foam from weathering and only modestly alters the foam's mechanical properties. When considering practical applications, the preservation of foam flexibility is very important. The ability to achieve this level of protection using a single bilayer deposited from water makes this a scalable system that could be used commercially. It is also likely that many of these beneficial properties could be realized with a variety of other two-dimensional nanomaterials (e.g., MoS_2), which could be the topic of future studies. A more fundamental understanding of the bonding/adhesion between these nanomaterials and various polymers is another important topic to be addressed in future work.

FTIR and TGA of h-BN before and after exfoliation, cone calorimetry results, and simulations of ^{11}B solid-state NMR spectra (PDF)

AUTHOR INFORMATION

Corresponding Authors

*E-mail: maude.jimenez@univ-lille.fr.

*E-mail: jgrunlan@tamu.edu.

ACKNOWLEDGMENTS

This study has received funding from the European Research Council (ERC) under the European Union's Horizon 2020 research and innovation program (grant agreement no. 670647/FireBarConcept/2014-2020) and is also based upon research supported by the Chateaubriand Fellowship of the Office for Science & Technology of the Embassy of France in the United States. The authors also acknowledge the Texas A&M Materials Characterization Facility (MCF), for infrastructural support, as well as Pierre Bachelet, Benjamin Dewailly, and Johan Sarazin for fire testing assistance and Bertrand Revel for NMR assistance. The TEM facility, SEM facility, and the electron probe microanalyzer (EPMA) facility in Lille (France) are supported by the Conseil Régional du Nord-Pas de Calais and the European Regional Development Fund (ERDF).

REFERENCES

(1) Biron, M. The Plastics Industry: Economic Overview. In *Thermosets and Composites - Technical Information for Plastics Users*; Elsevier Science: Oxford, NY, 2003; pp 31−144.

(2) Lefebvre, J.; le Bras, M.; Bastin, B.; Paleja, R.; Delobel, R. Flexible Polyurethane Foams: Flammability. *J. Fire Sci.* 2003, *21* (5), 343−367.

(3) Modesti, M.; Lorenzetti, A. FR Design for Foam Materials. In *Fire Retardancy of Polymeric Materials*; Wilkie, C., Morgan, A., Eds.; Taylor and Francis Group, LLC: Boca Raton, FL, 2010; pp 763−781.

(4) Shaw, S. Halogenated Flame Retardants: Do the Fire Safety Benefits Justify the Risks? *Rev. Environ. Health* 2010, *25* (4), 261−305.

(5) Holder, K. M.; Smith, R. J.; Grunlan, J. C. A Review of Flame Retardant Nanocoatings Prepared Using Layer-by-Layer Assembly of Polyelectrolytes. *J. Mater. Sci.* 2017, *52* (22), 12923−12959.

(6) Smith, R. J.; Holder, K. M.; Ruiz, S.; Hahn, W.; Song, Y.; Lvov, Y. M.; Grunlan, J. C. Environmentally Benign Halloysite Nanotube Multilayer Assembly Significantly Reduces Polyurethane Flamma- bility. *Adv. Funct. Mater.* 2018, *28* (27), 1703289.

(7) Pan, H.; Wang, W.; Pan, Y.; Song, L.; Hu, Y.; Liew, K. M. Formation of Layer-by-Layer Assembled Titanate Nanotubes Filled Coating on Flexible Polyurethane Foam with Improved Flame Retardant and Smoke Suppression Properties. *ACS Appl. Mater. Interfaces* 2015, *7* (1), 101−111.

(8) Yang, Y.-H.; Li, Y.-C.; Shields, J.; Davis, R. D. Layer Double Hydroxide and Sodium Montmorillonite Multilayer Coatings for the Flammability Reduction of Flexible Polyurethane Foams. *J. Appl. Polym. Sci.* 2015, *132* (14), 41767.

(9) Zhang, X.; Shen, Q.; Zhang, X.; Pan, H.; Lu, Y. Graphene Oxide-Filled Multilayer Coating to Improve Flame-Retardant and Smoke Suppression Properties of Flexible Polyurethane Foam. *J. Mater. Sci.* 2016, *51* (23), 10361−10374.

(10) Pan, H.; Pan, Y.; Wang, W.; Song, L.; Hu, Y.; Liew, K. M. Synergistic Effect of Layer-by-Layer Assembled Thin Films Based on Clay and Carbon Nanotubes To Reduce the Flammability of Flexible

Polyurethane Foam. *Ind. Eng. Chem. Res.* 2014, *53* (37), 14315−14321.
(11) Carosio, F.; Alongi, J. Ultra-Fast Layer-by-Layer Approach for Depositing Flame Retardant Coatings on Flexible PU Foams within Seconds. *ACS Appl. Mater. Interfaces* 2016, *8* (10), 6315−6319.
(12) Patra, D.; Vangal, P.; Cain, A. A.; Cho, C.; Regev, O.; Grunlan, J. C. Inorganic Nanoparticle Thin Film That Suppresses Flammability of Polyurethane with Only a Single Electrostatically-Assembled Bilayer. *ACS Appl. Mater. Interfaces* 2014, *6* (19), 16903−16908.
(13) Cain, A. A.; Plummer, M. G. B.; Murray, S. E.; Bolling, L.; Regev, O.; Grunlan, J. C. Iron-Containing, High Aspect Ratio Clay as Nanoarmor That Imparts Substantial Thermal/Flame Protection to Polyurethane with a Single Electrostatically-Deposited Bilayer. *J. Mater. Chem. A* 2014, *2* (41), 17609−17617.
(14) Luo, W.; Wang, Y.; Hitz, E.; Lin, Y.; Yang, B.; Hu, L. Solution Processed Boron Nitride Nanosheets: Synthesis, Assemblies and Emerging Applications. *Adv. Funct. Mater.* 2017, *27* (31), 1701450.
(15) Zhang, K.; Feng, Y.; Wang, F.; Yang, Z.; Wang, J. Two Dimensional Hexagonal Boron Nitride (2D-HBN): Synthesis, Properties and Applications. *J. Mater. Chem. C* 2017, *5* (46), 11992−12022.
(16) Zheng, Z.; Cox, M.; Li, B. Surface Modification of Hexgonal Boron Nitride Nanomaterials: A Review. *J. Mater. Sci.* 2018, *53*, 66−99.
(17) Song, W.-L.; Wang, P.; Cao, L.; Anderson, A.; Meziani, M. J.; Farr, A. J.; Sun, Y.-P. Polymer/Boron Nitride Nanocomposite Materials for Superior Thermal Transport Performance. *Angew. Chem., Int. Ed.* 2012, *51* (26), 6498−6501.
(18) Fu, L.; Wang, T.; Yu, J.; Dai, W.; Sun, H.; Liu, Z.; Sun, R.; Jiang, N.; Yu, A.; Lin, C.-T. An Ultrathin High-Performance Heat Spreader Fabricated with Hydroxylated Boron Nitride Nanosheets. *2D Mater.* 2017, *4* (2), 025047.
(19) Wu, Y.; Xue, Y.; Qin, S.; Liu, D.; Wang, X.; Hu, X.; Li, J.; Wang, X.; Bando, Y.; Golberg, D.; Chen, Y.; Gogotsi, Y.; Lei, W. BN Nanosheet/Polymer Films with Highly Anisotropic Thermal Conductivity for Thermal Management Applications. *ACS Appl. Mater. Interfaces* 2017, *9* (49), 43163−43170.
(20) Chen, J.; Huang, X.; Sun, B.; Wang, Y.; Zhu, Y.; Jiang, P. Vertically Aligned and Interconnected Boron Nitride Nanosheets for Advanced Flexible Nanocomposite Thermal Interface Materials. *ACS Appl. Mater. Interfaces* 2017, *9* (36), 30909−30917.
(21) Gu, J.; Lv, Z.; Wu, Y.; Guo, Y.; Tian, L.; Qiu, H.; Li, W.; Zhang, Q. Dielectric Thermally Conductive Boron Nitride/Polyimide Composites with Outstanding Thermal Stabilities via in-Situ Polymerization-Electrospinning-Hot Press Method. *Composites, Part A* 2017, *94*, 209−216.
(22) Yang, X.; Tang, L.; Guo, Y.; Liang, C.; Zhang, Q.; Kou, K.; Gu, J. Improvement of Thermal Conductivities for PPS Dielectric Nanocomposites via Incorporating NH2-POSS Functionalized NBN Fillers. *Composites, Part A* 2017, *101*, 237−242.
(23) Wang, Y.; Xu, L.; Yang, Z.; Xie, H.; Jiang, P.; Dai, J.; Luo, W.; Yao, Y.; Hitz, E.; Yang, R.; Yang, B.; Hu, L. High Temperature Thermal Management with Boron Nitride Nanosheets. *Nanoscale* 2018, *10* (1), 167−173.
(24) Teng, C.; Lin, Y.; Tan, Y.; Liu, J.; Wang, L. Facile Assembly of a Large-Area BNNSs Film for Oxidation/Corrosion-Resistant Coatings.
Adv. Mater. Interfaces 2018, *5* (19), 1800750.
(25) Li, J.; Gan, L.; Liu, Y.; Mateti, S.; Lei, W.; Chen, Y.; Yang, J. Boron Nitride Nanosheets Reinforced Waterborne Polyurethane Coatings for Improving Corrosion Resistance and Antifriction
Properties. *Eur. Polym. J.* 2018, *104*, 57−63.
(26) Mahvash, F.; Eissa, S.; Bordjiba, T.; Tavares, A. C.; Szkopek, T.; Siaj, M. Corrosion Resistance of Monolayer Hexagonal Boron Nitride on Copper. *Sci. Rep.* 2017, *7* (1), 42139.
(27) Kim, T. Y.; Song, E. H.; Kang, B. H.; Kim, S. J.; Lee, Y.-H.; Ju, B.-K. Hydrolyzed Hexagonal Boron Nitride/Polymer Nanocompo- sites for Transparent Gas Barrier Film. *Nanotechnology* 2017, *28* (12), 12LT01.
(28) Nguyen, H.-L.; Hanif, Z.; Park, S.-A.; Choi, B.; Tran, T.; Hwang, D.; Park, J.; Hwang, S.; Oh, D. Sustainable Boron Nitride Nanosheet-Reinforced Cellulose Nanofiber Composite Film with Oxygen Barrier without the Cost of Color and Cytotoxicity. *Polymers* 2018, *10* (5), 501.
(29) Cao, W.; Jiang, J.; Xie, X.; Pal, A.; Chu, J. H.; Kang, J.; Banerjee, K. 2-D Layered Materials for Next-Generation Electronics: Opportunities and Challenges. *IEEE Trans. Electron Devices* 2018, *65* (10), 4109−4121.
(30) Lin, Y.; Williams, T. V.; Xu, T.-B.; Cao, W.; Elsayed-Ali, H.E.; Connell, J. W. Aqueous Dispersions of Few-Layered and Monolayered Hexagonal Boron Nitride Nanosheets from Sonication-Assisted Hydrolysis: Critical Role of Water. *J. Phys. Chem. C* 2011, *115* (6), 2679−2685.
(31) Hu, Z.; Wang, S.; Chen, G.; Zhang, Q.; Wu, K.; Shi, J.; Liang, L. ; Lu, M. An Aqueous-Only, Green Route to Exfoliate Boron Nitride for Preparation of High Thermal Conductive Boron Nitride Nanosheet/Cellulose Nanofiber Flexible Film. *Compos. Sci. Technol.*
2018, *168*, 287−295.
(32) Liu, D.; Zhang, M.; He, L.; Chen, Y.; Lei, W. Layer-by-Layer Assembly Fabrication of Porous Boron Nitride Coated Multifunctional Materials for Water Cleaning. *Adv. Mater. Interfaces* 2017, *4* (16), 1700392.
(33) Olawoyin, R. Nanotechnology: The Future of Fire Safety. *Safety Science* 2018, *110*, 214−221.
(34) Massiot, D.; Fayon, F.; Capron, M.; King, I.; Le Calvé, S.; Alonso, B.; Durand, J.-O.; Bujoli, B.; Gan, Z.; Hoatson, G. Modelling One- and Two-Dimensional Solid-State NMR Spectra: Modelling 1D and 2D Solid-State NMR Spectra. *Magn. Reson. Chem.* 2002, *40* (1), 70−76.
(35) Wang, J.; Ma, F.; Sun, M. Graphene, Hexagonal Boron Nitride, and Their Heterostructures: Properties and Applications. *RSC Adv.* 2017, *7* (27), 16801−16822.
(36) Ortiz, D.; Pochat-Bohatier, C.; Cambedouzou, J.; Bechelany, M.; Miele, P. Exfoliation of Hexagonal Boron Nitride in Liquide Phase by Ion Intercalation. *Nanomaterials* 2018, *8*, 716.
(37) Xie, S.-Y.; Wang, W.; Fernando, K. A. S.; Wang, X.; Lin, Y.; Sun, Y.-P. Solubilization of Boron Nitride Nanotubes. *Chem. Commun.* 2005, *0*, 3670−3672.
(38) Lin, Y.; Williams, T.; Cao, W.; Elsayed-Ali, H.; Connell, J. Soluble, Exfoliated h-BN Nanosheets. *J. Phys. Chem. C* 2010, *114*, 17434−17439.
(39) Kumari, S.; Sharma, O.; Khatri, O. Alkylamine-Functionalized Hexagonal Boron Nitride Nanoplatelets as a Novel Material for the Reduction of Friction and Wear. *Phys. Chem. Chem. Phys.* 2016, *18*, 22879−22888.

(40) Marchetti, P. S.; Kwon, D.; Schmidt, W. R.; Interrante, L. V.; Maciel, G. E. High-Field Boron-11 Magic-Angle Spinning NMR Characterization of Boron Nitrides. *Chem. Mater.* 1991, *3* (3), 482−486.

(41) Gervais, C.; Babonneau, F. High Resolution Solid State NMR Investigation of Various Boron Nitride Preceramic Polymers. *J. Organomet. Chem.* 2002, *657* (1−2), 75−82.

(42) Gervais, C.; Framery, E.; Duriez, C.; Maquet, J.; Vaultier, M.; Babonneau, F. 11B and 15N Solid State NMR Investigation of a Boron Nitride Preceramic Polymer Prepared by Ammonolysis of Borazine. *J. Eur. Ceram. Soc.* 2005, *25* (2−3), 129−135.

(43) Wang, J.; Zhang, D.; Zhang, Y.; Cai, W.; Yao, C.; Hu, Y.; Hu, W. Construction of Multifunctional Boron Nitride Nanosheet towards Reducing Toxic Volatiles (CO and HCN) Generation and Fire Hazard of Thermoplastic Polyurethane. *J. Hazard. Mater.* 2019, *362*, 482−494.

(44) Lazar, S.; Carosio, F.; Davesne, A.-L.; Jimenez, M.; Bourbigot, S.; Grunlan, J. Extreme Heat Shielding of Clay/Chitosan Nanobrick Wall on Flexible Foam. *ACS Appl. Mater. Interfaces* 2018, *10* (37), 31686−31696.

(45) Podsiadlo, P.; Kaushik, A. K.; Arruda, E. M.; Waas, A. M.; Shim, B. S.; Xu, J.; Nandivada, H.; Pumplin, B. G.; Lahann, J.; Ramamoorthy, A.; Kotov, N. A. Ultrastrong and Stiff Layered Polymer Nanocomposites. *Science* 2007, *318* (5847), 80−83.

(46) Podsiadlo, P.; Tang, Z.; Shim, B. S.; Kotov, N. A. Counterintuitive Effect of Molecular Strength and Role of Molecular Rigidity on Mechanical Properties of Layer-by-Layer Assembled Nanocomposites. *Nano Lett.* 2007, *7* (5), 1224−1231.

(47) Rosu, D.; Rosu, L.; Cascaval, C. N. IR-Change and Yellowing of Polyurethane as a Result of UV Irradiation. *Polym. Degrad. Stab.* 2009, *94* (4), 591−596.

(48) Tran, T. V.; Abedin, F.; Usta, A.; Asmatulu, R. Polyurethane Nanocomposite Coating with Silanized Graphene and Hexagonal Boron Nitride as Nanoadditives for Improved Resistance against Ultraviolet Degradation. *J. Compos. Mater.* 2019, *53* (10), 1387−1399.